American Journal of Aging Science and Research

Roterman, Am J Aging Sci Res. 2024;4(1):5-14.

Commentary

Environmental determinants for protein structuring and amyloid transformation

Roterman I[1,*], Stapor K[2], Dułak D[3], Konieczny L[4]

[1]Department of Bioinformatics and Telemedicine, Jagiellonian University -Medical College, 30-688 Krakow, Medyczna 7 Poland

[2]Faculty of Automatic, Electronics and Computer Science, Department of Applied Informatics, Silesian University of Technology, Akademicka 16, 44-100 Gliwice, Poland

[3]ABB Business Services Sp. z o.o. ul. Żegańska 1, 04-713 Warszawa, Poland

[4]Chair of Medical Biochemistry, Jagiellonian University - Medical College, 31-034 Krakow, Kopernika 7, Poland

*Author for correspondence:
Email: myroterm@cyf-kr.edu.pl

Received date: July 18, 2024
Accepted date: August 08, 2024

Citation:Roterman I, Stapor K, Dułak D, Konieczny L. Environmental determinants for protein structuring and amyloid transformation. Am J Aging Sci Res. 2024;4(1):5-14.

Abstract

Amyloid transformation under laboratory conditions is achieved by shaking an aqueous solution of any protein. The shaking time varies significantly, demonstrating the variable degree of ease of structural transformation in a given protein. The structural specificity that distinguishes amyloid forms from biologically active proteins is the flatness (two-dimensionality) of the form of each chain in the amyloid fibril. The 2D feature, given the globular and therefore 3D structure of biologically active proteins, is an object of analysis in the search for factors favoring amyloid transformation. The use of a modified fuzzy oil drop model (FOD-M) enables this transformation to be mathematically expressed. The mathematical expression is directly related to the shaking conditions, while leaving open the question of an environmental factor under physiological conditions that causes a conformational change resulting in a 2D structure of the polypeptide chain. The examples expressing the environmental prerequisites demonstrated in the current review show the dependence of structuring on the external force field.

Keywords: Amyloid, Transthyretin, VL domain IgG, Synuclein, Enzymes, Hydrophobicity, External force field, Structural changes, Amyloid transformation

Introduction

The issue of structural transformation of proteins to the amyloid form is a predominant question discussed in the literature [1-4]. This discussion began with the identification of proteins referred to as prions that are the starting agent for structuring into fibrils [5-7]. Multiple medical findings provide valuable data for experimental studies, the results of which are evident in the availability of many amyloid fibril structures in the Protein Data Bank (PDB) resources [8]. No explicit model has been proposed for the process of structural transformation leading to pathological fibrils causing (if localized in the brain) neurodegenerative diseases [9-11]. The effect of hereditary mutations on the ease of transformation to the amyloid form has been identified [12,13], although the presence of mutations is not a prerequisite for amyloid transformation, as demonstrated by an experimental method of producing amyloid structures from arbitrary proteins by shaking [14,15]. This paper proposes a mathematical model to express the effects of an external force field allowing the level of change in environmental conditions on the structuring of biologically active proteins, including those considered to be pathological [16].

Model Description

By treating amino acids as bi-polar molecules with a varying ratio of polar to hydrophobic parts, it can be assumed that the polypeptide chain in an aqueous environment tends towards an optimal organization involving isolation of the hydrophobic parts in the center of the protein and exposure of the polar residues for optimal contact with polar water [17]. Such a tendency is observed in the micelle arrangement, which represents an idealized arrangement with a perfect organization corresponding

to the optimum arrangement in a polar water environment. The hydrophobicity distribution in this arrangement – the idealized micelle-like one – can be expressed by a 3D Gaussian function spanned over the body of the protein:

$$T_i = \frac{1}{\sum_{i=1}^{N} T_i} \exp\left[\frac{-(x_i-\bar{x})^2}{2\sigma_x^2}\right] \exp\left[\frac{-(y_i-\bar{y})^2}{2\sigma_y^2}\right] \exp\left[\frac{-(z_i-\bar{z})^2}{2\sigma_z^2}\right] \quad \text{Eq. 1.}$$

The magnitude of the parameters σ_x , σ_y and σ_z corresponds to the size and shape of the protein. The maximum of this function is at the central point of the ellipsoid (**Figure 1A**). The distribution expressed by Eq. 1 is the presence of a hydrophobic core – high hydrophobicity values concentrated in the central part of the ellipsoid, with a gradual reduction in hydrophobicity levels until zero at the surface (**Figure 1A**).

The $\sum_{i=1}^{N} T_i$ expresses the sum of all *Ti* making all *Ti* values normalized.

The extent of validity of such an assumption of micelle-like structuring for proteins is convincing by determining the actual hydrophobicity distribution resulting from hydrophobic interactions between amino acids present in the protein. Here, the function by M. Levitt [18] can be applied.

$$O_i = \frac{1}{\sum_{i=1}^{N} O_i} \sum_j \begin{cases} (H_i^r + H_j^r)(1 - \frac{1}{2}(1 - \frac{1}{2}(7(\frac{r_{ij}}{c})^2 - 9(\frac{r_{ij}}{c})^4 + 5(\frac{r_{ij}}{c})^6 - (\frac{r_{ij}}{c})^8 - (\frac{r_{ij}}{c})^8)), for r_{ij} \le c \\ 0, for r_{ij} > c \end{cases} \quad \text{Eq. 2.}$$

with c - the cut-off of 9 Å and r_{ij} - the distance between the positions of the effective atoms (the averaged position of the atoms comprising the amino acid). The magnitude of the effect also depends, of course, on the intrinsic hydrophobicity H^r of each amino acid (any scale can be used [19]). The $\sum_{i=1}^{N} O_i$ expresses the sum of all O*i* making all O*i* values normalised.

A comparison of the idealized distribution (Eq. 1.) denoted as T, and the observed distribution **(**Eq**. 2)**, denoted as O, facilitates an assessment of the degree of organization against a micelle-like distribution. This assessment is done using the divergence entropy introduced by Kullback-Leibler [20].

$$D_{KL}(P \mid Q) = \sum_{i=1}^{N} P_i \log_2 \frac{P_i}{Q_i} \quad \text{Eq. 3.}$$

with *Pi* being the distribution of interest – the distribution O in our analysis; the distribution *Q* is the reference distribution – the distribution *T* in our analysis.

Using the notation introduced in this paper the eq. 3 takes the form:

$$D_{KL}(O \mid T) = \sum_{i=1}^{N} O_i \log_2 \frac{O_i}{T_i} \quad \text{Eq. 4.}$$

Before applying Eq. 4, both distributions *T* and *O* must be normalized.

The value $D_{KL}(O|T)$ is not a quantitatively interpretable quantity (D_{KL} expresses entropy). Therefore, a second reference distribution denoted as R is introduced, where each effective atom is described by the value *Ri = 1/N*, with N being the number of amino acids in the protein. The distribution R represents an arrangement completely opposite to the distribution T. No local concentration of hydrophobicity is present in the distribution R. Its distribution is uniform across the protein body.

A comparison of the $D_{KL}(O|T)$ and $D_{KL}(O|R)$ (the reference distribution T is substituted by R in eq. 4) distributions enables an assessment of the degree of similarity of the distribution O versus two reference distributions of an extremely different nature, T and R.

To avoid the need to operate with two quantities to describe the same arrangement, the parameter *RD* (Relative Distance) is introduced, defined as follows:

$$RD = \frac{D_{KL}(O \mid T)}{D_{KL}(O \mid T) + D_{KL}(O \mid R)} \quad \text{Eq. 5.}$$

The interpretation of the RD value follows: RD < 0.5 indicates the presence of a hydrophobic core, RD > 0.5 indicates an organization different from a micelle-like arrangement.

Using this defined criterion for assessing the structuring of a given protein, it is possible to determine the degree of similarity of the distribution O with respect to the distributions T and O, which amounts to determining the degree of presence of a micelle-like arrangement in the protein.

The distribution is characteristic of proteins folding and performing their biological activity in an aqueous environment. However, this activity is also displayed in other environments. The opposite of the aqueous environment is the cell membrane environment. Here, the exposure of hydrophobic residues is expected for a favorable stabilizing interaction with the hydrophobic cell membrane and — in the case of ion channels — the presence of polar groups at the center. Therefore, a function (*Mi*) complementary to Eq. 1 is proposed for the expression of this opposite arrangement.

$$Mi = 1\text{-}Ti \quad \text{Eq. 6.}$$

In practice, this function is expressed by:

$$Mi = T_{MAX} - Ti \quad \text{Eq. 7.}$$

With T_{MAX} being the maximum value of Eq. 1.

Analysis of numerous proteins showed that the distribution in membrane proteins is expressed by:

$$Mi = Ti + \{K^* [T_{MAX}\text{-}Ti]n\}n \quad \text{Eq. 8.}$$

with the subscript *n* indicating normalization.

The interpretation of the function determined with this equation is as follows:

1. The presence of an aquatic environment is common. The component in the form of Ti expresses the need for the presence of an aqueous environment to drive the structuring of the final active protein in the aqueous environment.
2. The presence of the complementary function indicates the impact of a non-aqueous environment.
3. The magnitude of the parameter K expresses the degree to which a typical arrangement resulting from an aqueous external force field should be modified by external factors.

4. Thus, the value of the parameter K indicates the degree of deformation of the micelle-like arrangement resulting from the influence of non-aqueous factors including hydrophobic factors in particular.

A graphical representation of the model in question is shown in **Figure 1**.

In A and D – the values on x-axis are expressing the normalized variable, which for Gauss function takes the range -3σx to +3σx. The unit on the axis is 1 standard deviation – σx.

The graphic presentation of protein encapsulation in ellipsoid is also shown in (**Figure 2).** The investigator with three detectors is registering the level of theoretical, expected hydrophobicity in form of micelle-like with central concentration of hydrophobicity and with low hydrophobicity on the surface (according to eq. 1 – the blue detector). The closer to the center is the detector the higher is the level of hydrophobicity (blue line). The real distribution of hydrophobicity appears to be different (red line detected by red detector) (eq. 2).

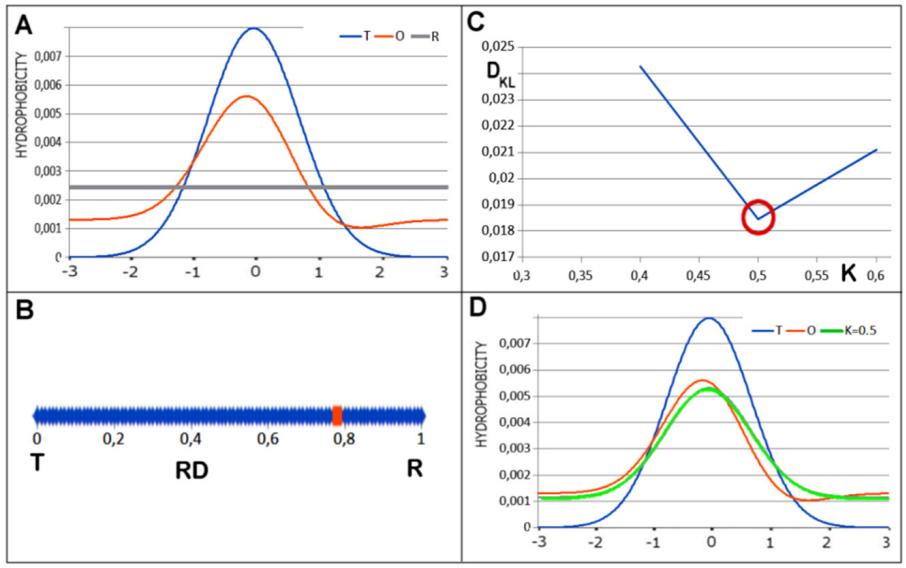

Figure 1. Graphical representation of the model reduced to 1D for ease of reference: **A** – juxtaposition of distributions: T (blue), O (red), R (gray). **B** – the RD value determined for the set in A is 0.785 and so the distribution O does not represent an arrangement with a hydrophobic core present. **C** – determination of K, the minimum value of $D_{KL}(O|M)$. **D** – juxtaposition of profiles: T, O and M with K=0.5.

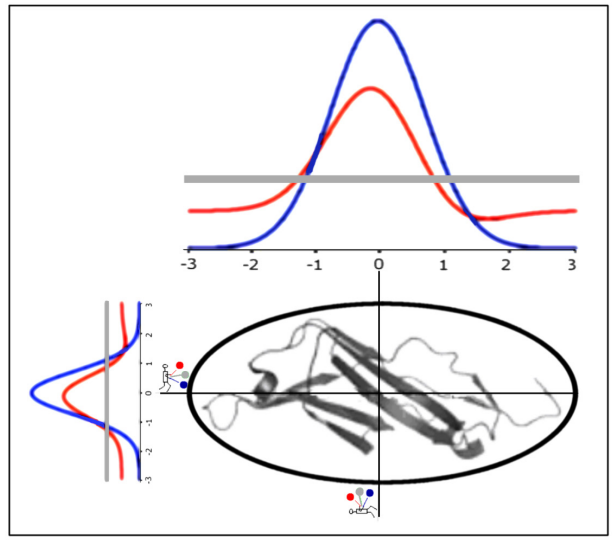

Figure 2. The visualization of protein encapsulation in ellipsoid expressed by 3D Gauss function (in the presentation reduced to 2D due to graphic limitations). The detectors (in the hand of investigator) designated for different registrations visualize the three distributions T, O and R. The Gauss function is expressed by parameters σ: σx on the horizontal upper profiles and σy on the vertical profiles. These parameters are shown on appropriate axes. The specificity of Gauss function is to be limited for the scale -3σ to +3σ (tree sigma rule).

Thus, the empirical distribution can be compared with the idealized one with centric hydrophobic core (T distribution) and also with the opposite distribution deprived on any hydrophobicity differentiation (grey line registered by grey detector). The comparison with both idealized distributions: T and R can be expressed by *RD* (eq. 5 (**Figure 1B**). The RD value, which is high for this example suggests the absence of hydrophobic core (the O distribution is closer the R distribution).

Figure 2 visualizes the assessment of O distribution in respect to idealized Gauss distribution (T) and idealized unified distribution (R). The eq. 8 introduces definition of the modified distribution M. The M distribution is the closest one (for observed distribution) to represent the idealized, ordered hydrophobicity distribution in form modified by environment. It is shown in **Figure 3** that the M distribution (green detector in the hand of investigator) is the idealized one retraced by observed distribution (red line). The folding process is running according to external conditions (parameter K measures the specificity of environment) reaching the distribution which fits the M distribution (green line) and doesn't fit T (blue line) distribution.

Analysis of numerous proteins identified proteins with a distribution highly compatible with a micelle-like distribution — these are down-hill, fast-folding, ultra-fast-folding, and antifreeze type II proteins [21]. The identification of the proteins demonstrates the validity of the basic assumption that the folding process in an aqueous environment is a micellization process.

The identification of proteins with gradually increasing values of the parameter K expresses differentiated external force fields that lead to a specific type of hydrophobicity distribution in the protein body, including R-type distribution. The contribution of chaperones is an example of deliberately altered external force field conditions, which include prefoldin [22]. The presence of prefoldin, for example, is intended to prevent rippling resulting solely from the presence of surrounding polar water. The involvement of chaperonin in the folding process is also a classic example. Chaperonin is the provider of a distinct local environment for the protein, whose expected hydrophobicity distribution is distinct from the centric nucleus, providing biological function in numerous cases. An overview of the proteins is given, for example, in [23-25].

The conclusion drawn from the model discussed above is the structure of the protein is encoded in the amino acid sequence in such a way that the appropriate degree and type of dissimilarity to the idealized micelle-like arrangement is achieved. Micelle-like structuring cannot exhibit any activity due to the repetitive and symmetrical nature of the arrangement. Local incompatibility with the micelle-like arrangement is needed for activity to occur in this specificity. Therefore, the following is proposed: "A protein is an intelligent micelle", which has information encoded in a local defect that tells of the potential to interact with other molecules or form complexes [26].

This paper continues the interpretation of examples representing the spectrum of opportunities and diversity resulting from sequence variability on the one hand, but also from the variability of the external force field, which varies in the organism — e.g. the lysosome or even gastric environments are very different from the physiological aquatic environment. The membrane environment is also an example of a different environment, where appropriately folded proteins are stably anchored and can exhibit biological activity.

In this arrangement, amyloid proteins occupy a very highly specific place, as the term micellization itself carries the concept of three-dimensionality that the flat single chain-components of amyloid fibrils do not represent.

The applicability of the model seems to be unlimited. Any protein may be encapsulated by appropriate 3D Gauss function. However, the proteins of very complicated structure – far from globular ones – fitted to regular ellipsoid may introduce some discrepancies. However, the status of protein parts – like domains or

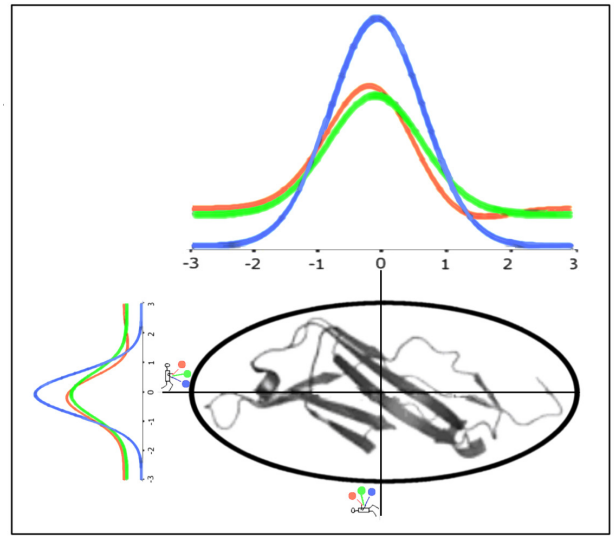

Figure 3. The protein encapsulated in ellipsoid (3D Gauss function – on presentation limited to 2D) appears to represent the observed hydrophobicity distribution which retraces the external force field expressed by M function (green line). The three detectors register the levels of hydrophobicity in protein. The best fit for observed distribution (red one) is the M distribution (green). The value of K for M distribution informs what is the degree of the environment difference in respect to polar water one (blue line).

subjectively defined structural units – can be evaluated in respect to the hydrophobicity organization. Amyloid fibrils are characterized by large σx parameter due to the significant elongation of the fibril structure.

Examples of Proteins of Different Status (RD and K) with Biological Activity

The proteins selected to represent different status as expressed by FOD-M model are characterized by the set of profiles: T, O and M for appropriate K value. The 3D structure of each protein is also shown. Additionally, the upper right insets visualize the changes of M function according to changed external conditions expressed by K parameter. The lower maximum of the Gauss function the higher influence of non-polar environment causing the hydrophobicity distribution less similar to micelle-like (gradual disappearance of hydrophobic core and increase hydrophobicity on the surface of protein).

Down-hill proteins and antifreeze type II proteins as well as numerous domains treated as individual structural units show an ordering consistent with a micelle-like arrangement with low RD and K values.

A distribution with a value close to K=0.0 and therefore consistent with the 3D Gaussian function system was identified for mannose-6-phosphate isomerase from *Helicobacter pylori* (PDB ID - 2QH5) [27]. The parameters for this protein follow: RD=0.419 and K=0.3. The RD value suggests the presence of a hydrophobic nucleus as seen in the set of profiles T and O **(Figure 4).** The low value of K = 0.3 suggests folding of this protein as a process driven by the aqueous environment directing the structuring towards a micelle model. Profile M for K=0.3 (**Figure 4** - inset - top right) differs little from the distribution T.

In addition, many prion proteins show a highly organized structure with a hydrophobic nucleus present. An example is the major prion protein domain prp (121-231) derived from a mouse (PDB ID - 1AG2 [28]. A hydrophobic nucleus structure can be seen, which stabilizes the overall structure **(Figure 5)**. It is therefore surprising that a structure stabilized by the presence of a well-formed hydrophobic nucleus undergoes a radical change leading to an amyloid fibril form [29]. The RD value for the protein is 0.454 with K=0.3.

An example of a protein with the status expressed by RD = 0.451 and K=0.5 is the giardia guanine phosphoribosyl transferase, or the E.C.1. enzyme with 219 amino acids in the chain (PDB ID - 1DQP [30]. The degree of agreement of the distribution O against the distribution T and the determined optimal distribution M for this protein is shown in **(Figure 6** – inset – top right).

The juxtaposition of the profiles T and O indicates the location of the catalytic residues in the cavity (the local hydrophobicity deficit) with the exception of position 97Y, which is at the surface. The inset **(Figure 6 –** top right) reveals a changing profile for the modification resulting from the contribution of factors altering the polar water environment. These changes can be tracked by comparing the graphs shown in the insets in **Figures 4 and 5** and the inset in **Figure 6**.

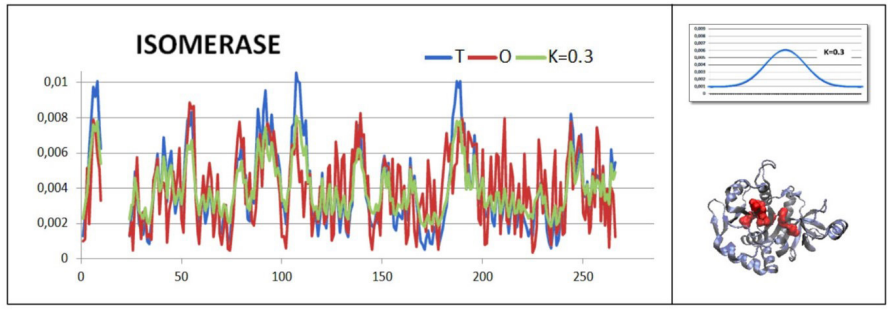

Figure 4. Characterization of the mannose-6-phosphate isomerase from *Helicobacter pylori*: a set of profiles T, O and M with K=0.3 together with a 3D presentation highlighting (in red) amino acids that display local maxima with a compatible high hydrophobicity value for the distributions T and O. Inset – top right – plot of the profile of the idealized distribution reduced to 1D, altered by K=0.3.

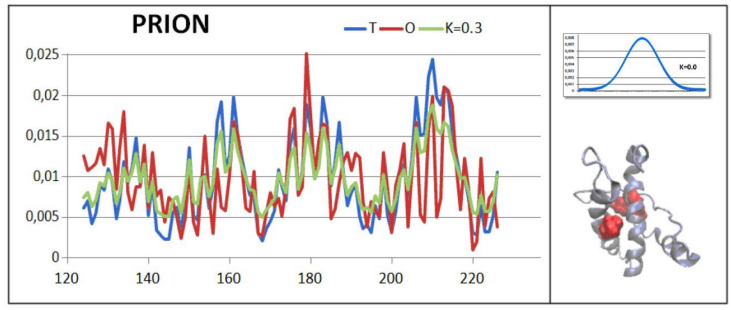

Figure 5. Characterization of the major prion protein domain prp (121-231) from a mouse: a set of profiles T, O and M for K=0.3 together with a 3D presentation highlighting (in red) the amino acids showing local maxima with a high hydrophobicity value consistent for distributions T and O. Inset – top right – plot of the profile of the idealized distribution reduced to 1D, with K=0.0. A profile for K=0.0 is provided for comparison to a profile with K=0.3 (**Figure 4** – see the inset).

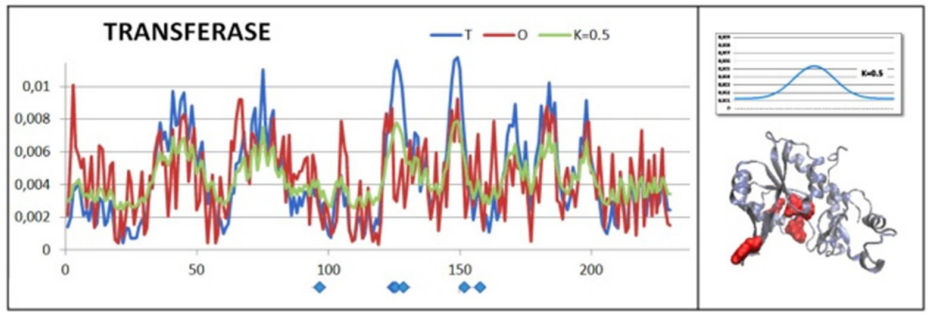

Figure 6. Characterization of giardia guanine phosphoribosyltransferase: a set of profiles T, O and M for K=0.5 together with a 3D presentation in which the catalytic amino acids are highlighted (in red; their positions in the chain sequence are highlighted on the horizontal axis with blue diamonds). Inset – top right – plot of the profile of the idealized distribution reduced to 1D, with K=0.5.

Another example illustrating the status with K=1.0 is the membrane protein bacteriorhodopsin (PDB ID - 1BM1) [31]. Here, the impact on significant dissimilarity to the conditions imposed by the water environment is clearly visible. Residues showing a deficit in hydrophobicity are present (the residues in blue on 3D presentation **– Figure 7).** These are positions with Oi levels significantly lower than expected against the expected high Ti values **(Figure 7)** These residues are identified as building cavities for a retinal bonding. Residues exhibiting redundant hydrophobicity are also evident – the residues that are in direct contact with the hydrophobic membrane **(Figure 7** – 3D presentation – see the residues in red).

The dissimilarity of the distribution O vs. the idealized distribution T is illustrated by the set of profiles T, O and M. A local excess of hydrophobicity vs. the expected low levels is evident — this applies to sections and surface positions **(Figure 7).** Fragments with a highlighted deficit in hydrophobicity are visible, indicating the presence of a retinal-bonding cavity **(Figure 7).** The status of the bacteriorhodopsin in question is expressed by the values of these parameters: RD=0.712 and K=1.0.

A high degree of distinctiveness of the decomposition O against T is shown by the enzyme E.C.1.4.3.21-primary-amine oxidase (PDB ID - 1AV4) [32]. It is a 620 amino acid chain protein within which three domains are distinguished: Dom1 (9-95), Dom2 (96-203) and Dom3 (204-627). The status of this protein is determined by the values: RD=0.701 and K= 1.3. The domains treated as individual structural units are characterized by the following parameters Dom1: RD=0.618, K =0.5 ; Dom2 : RD=0.493 K= 0.4; Dom3 : RD=0.630 K = 0.6.

The juxtaposition of profiles T and O for the entire chain reveals a significant mismatch in the distributions T and O (**Figure 8**). In addition, profile M approaches an R-type distribution. This implies the generation of the structure in isolation from the polar water environment. Additionally, it can be speculated that Dom2 formed in an aqueous environment obtaining a hydrophobic nucleus and a polar shell. In contrast, Dom1 and Dom3 required the presence of factors that alter external force field conditions.

To visualize the variation in the status of the domains, sets of profiles T, O and M are also shown for the respective K values for each domain treated as an individual structural unit (a 3D Gaussian function spanning each domain independently) **(Figure 9**).

Figure 9 visualizes the variation in the status of individual domains. This is another example of the different degrees of dissimilarity from the micelle-like arrangement. The various forms and degrees of mismatch between distributions O and the corresponding distributions T exemplify the capabilities of the FOD-M model to assess the status of a structural unit against an idealized hydrophobic nucleus and to assess the possible contribution of environmental factors driving the folding of the structural unit.

The distributions shown in the 1D form (see insets in **Figure 4** to **Figure 8)** visualize the variation of the external force field, which, as the K value increases, approaches the distribution R. The

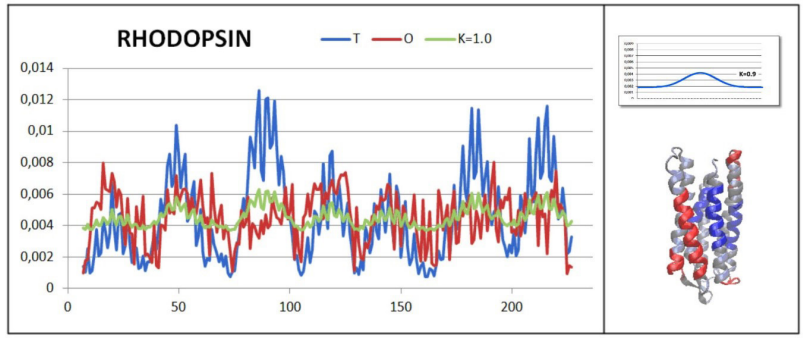

Figure 7. Characterization of bacteriorhodopsin: a set of profiles T, O and M with K=1.0, together with a 3D presentation highlighting (in red) the amino acids showing excess hydrophobicity remaining in contact with the membrane and (in blue) hypo-hydrophobic residues in the retinal bonding pocket. Inset – top right – plot of the profile of the idealized distribution reduced to 1D, with K=0.9.

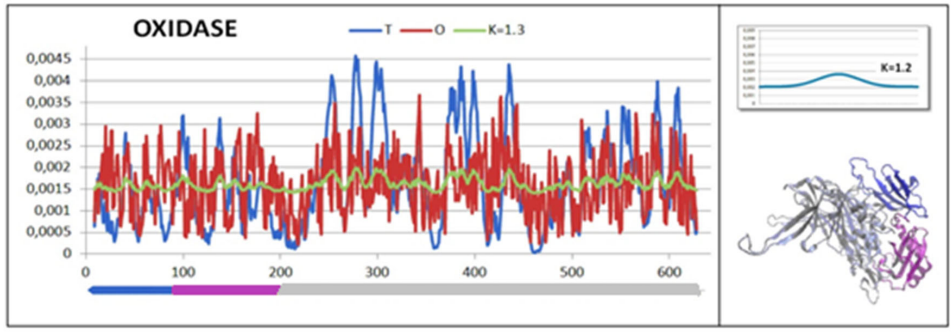

Figure 8. Characteristics of E.C.1.4.3.21-primary-amine oxidase: a set of profiles T, O and M for K=1.3 together with a 3D presentation in which the domains are highlighted: Dom1 – blue; Dom2 – purple; Dom3 – grey. The fragments building the respective domains are also shown on the horizontal axis together with a set of profiles T, O and M, highlighted by colors like on the 3D presentation. Inset – top right – plot of the profile of the idealized distribution reduced to 1D, with K=1.2.

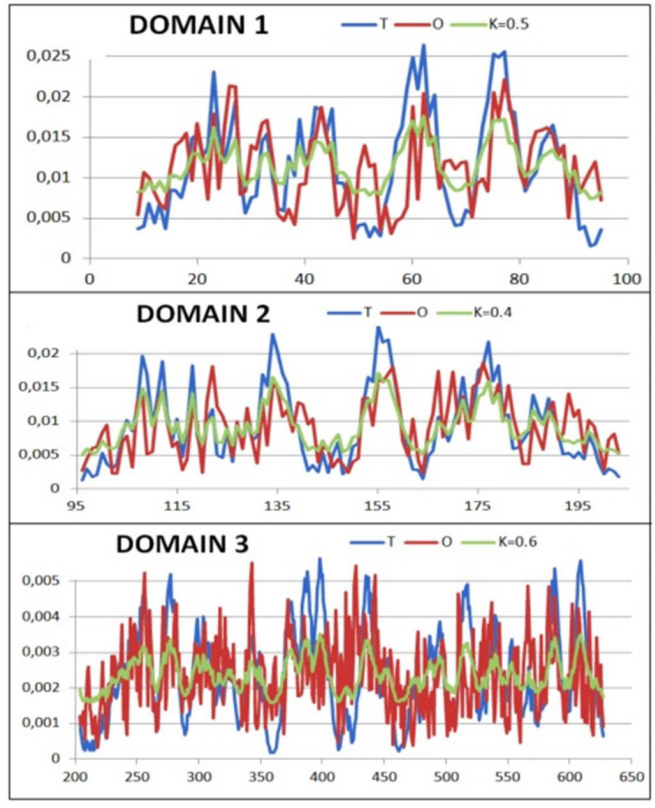

Figure 9. Juxtaposition of profiles T, O and M for the corresponding K value for domains present in primary-amine oxidase.

distribution R is an example of an environment completely isolated from the influence of polar water. Such a different environment is provided by chaperonins, where the folding protein isolated from contact with water adjusts its organization of hydrophobicity to the surrounding external force field [22,23]. A comparative analysis with the status of amyloid proteins indicates the involvement of extrinsic factors shaping the type of folding in question, including the flat (2D) structure of the chain-components of amyloid fibrils in particular. The proteins discussed here provide an overview of the possible environmental changes found in biologically active proteins.

Specificity of Amyloid Structures

The examples presented are intended to indicate the role of environmental factors in protein structuring processes. Using the FOD-M model, an assessment of the transthyretin amyloid fibril status (**Figure 10**) and the VL domain of IgG **(Figure 11)** shows an up-regulation of the RD and K values relative to the status these proteins demonstrate in the native structure. This implies the need for a factor that changes the external force field from aqueous to one modified by factors that increase the parameter RD and K

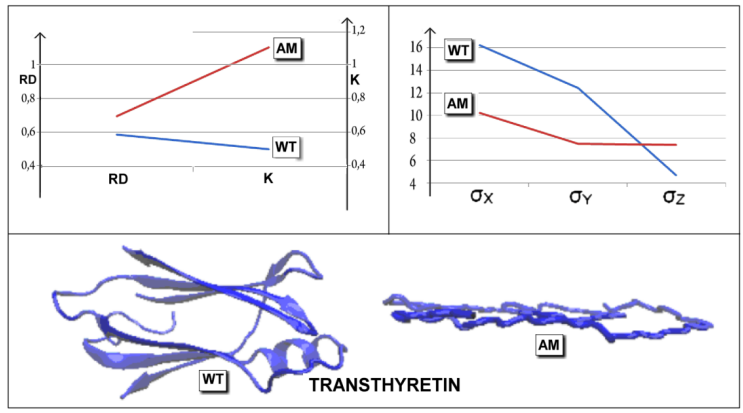

Figure 10. Juxtaposition of the parameters RD and K as well as σ_x, σ_y and σ_z for the native (WT) and amyloid (AM) forms of transthyretin together with a 3D presentation showing significant flattening of the chain structure as a component of the amyloid fibril.

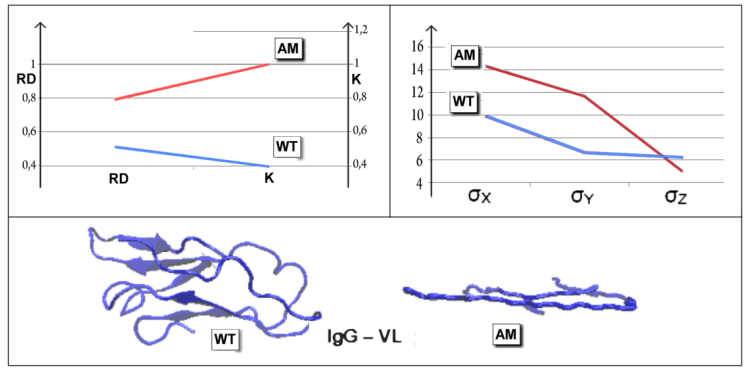

Figure 11. Juxtaposition of the parameters RD and K as well as σ_x, σ_y and σ_z for the native (WT) and amyloid (AM) forms of the VL domain of IgG together with a 3D presentation showing significant flattening of the chain structure as a component of the amyloid fibril.

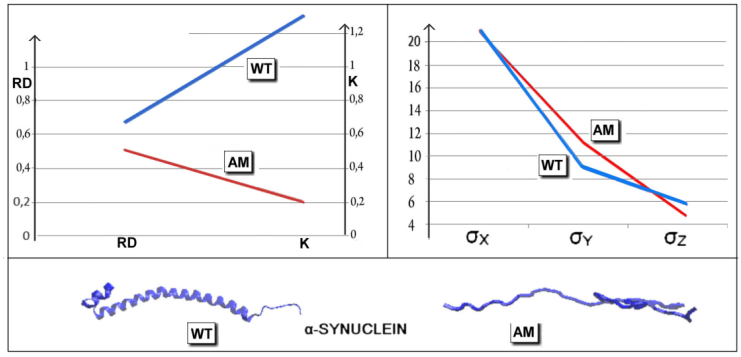

Figure 12. Juxtaposition of the parameters RD and K as well as σ_x, σ_y and σ_z for the native (WT) and amyloid (AM) forms of α-synuclein together with a 3D presentation showing flattening of the chain structure as a component of the amyloid fibril. The opposite relationship of RD and K for the native and amyloid forms of this protein to the previous examples can be seen.

values. This undoubtedly implies the involvement of external factors directing the amyloid transformation process [33].

The amyloid α-synuclein transformation represents changes of the opposite nature in the form of reduced RD and K parameter values for amyloid against the native structure [34-39] **(Figure 12)**. The native structure of the protein is described by very high RD and K values (α-synuclein is associated with the axon terminals of presynaptic neuron, which constitutes a specific permanent chaperone). The presence of an external force field in the form of a presynaptic neuron imposes a structure far from that favored by the aquatic environment. Liberation from these conditions imposed by the external force field (axon terminals of presynaptic neuron) causes α-synuclein in an aqueous environment to take the form of

an amyloid that fulfils the conditions of a micelle-like arrangement [17] **(Figure 12).**

An important feature of the amyloid structure is the flat (2D) form of the single chains, the components of amyloid fibrils. The proposed model describing the shape and size of a given protein by means of a 3D Gaussian function uses the parameters σ_x, σ_y and σ_z. It thus becomes possible to assess the change in shape and size of the chain in the native (WT) form against the form present in the amyloid fibril. **Figures 11 and 12** visualize these changes in the 3D form but also by means of changes in the values of the parameters σ_x, σ_y and σ_z. Each time, the value of the parameter σ_z decreases. In addition to the decreasing value of the parameter σ_z, a significant variation in the values of the other σ_x and σ_y is evident. The comparable values of σ_x, σ_y and σ_z express the globular (often even close to spherical) shape of the protein. A change in the ratio between the values of these parameters, e.g. a significant increase inσ_x, indicates the globular structure disappears.

The decreasing value of σ_z is justified by the nature of the experimental process of obtaining amyloids from many proteins, which is shaking. The process of shaking is to increase the presence of the air/water interphase, of which the 2D form is an essential feature. The emergence of air/water interphase in an organic body does not appear to be possible. This leaves open the question of the factor that introduces this type of conditioning under in vivo conditions, including in the brain tissue of homo sapiens in particular. The question of the factor introducing a preference for 2D structuring (which does not appear to be of a chemical nature) remains open.

Summary

The participation of external conditions in amyloid transformation seems to be obvious. The introduction of the parameter K in FOD-M model allows quantitative assessment of environmental changes. This parameter can be interpreted as representing the changed external force field supporting the structuralization preferable for individual chain to construct the amyloid fibril. The accordance between 2D model with 2D specificity of air/water interface may explain the effects of the increase of the interface of this type. However, this condition has so far no representation in any form of physiological specificity playing similar role in natural conditions.

The only therapeutic project based on the discussed model is the solution analogical to solenoids termination. The specificity of solenoid structure (for some aspects very similar to amyloids) theoretically allows the construction of very long (if not infinitely long) fibril-like construction. This process is prohibited in the form of terminals playing the role of natural stoppers. The short helices oriented diameter-like localized at the end of solenoid eliminate the complexation of the next solenoid. Additionally, the status of these helices together with the terminal fragment of solenoid represent the micelle-like construction allowing water penetration lowering the probability to paste the next solenoid molecule [40,41]. This model does not eliminate the source of amyloid transformation. This method may stop the propagation of fibrils.

The applicability of the discussed model to various groups of proteins: enzymes [25], assisted folding process [22-24], membrane proteins [42], water soluble proteins [21], homology proteins [43], CASP models evaluation [44], protein-protein interaction [26], intrinsically disordered proteins [45], hypothesis of COVID-19 pandemic [46] makes this model promising. Identification of cavity (potential locus for substrate or ligand binding) and local exposure of hydrophobicity as potential place for complexation makes the model applicable also in drug design discipline.

References

1. Leisi EV, Barinova KV, Kudryavtseva SS, Moiseenko AV, Muronetz VI, Kurochkina LP. Effect of bacteriophage-encoded chaperonins on amyloid transformation of α-synuclein. Biochem Biophys Res Commun. 2022 Sep 24;622:136-42.
2. Navalkar A, Pandey S, Singh N, Patel K, Datta D, Mohanty B, et al. Direct evidence of cellular transformation by prion-like p53 amyloid infection. J Cell Sci. 2021 Jun 1;134(11):jcs258316.
3. Toyama BH, Weissman JS. Amyloid structure: conformational diversity and consequences. Annu Rev Biochem. 2011;80:557-85.
4. Cao Y, Mezzenga R. Food protein amyloid fibrils: Origin, structure, formation, characterization, applications and health implications. Adv Colloid Interface Sci. 2019 Jul;269:334-56.
5. Prusiner SB. Novel proteinaceous infectious particles cause scrapie. Science. 1982 Apr 9;216(4542):136-44.
6. Spagnolli G, Requena JR, Biasini E. Understanding prion structure and conversion. Prog Mol Biol Transl Sci. 2020;175:19-30
7. Legname G, Moda F. The Prion Concept and Synthetic Prions. Prog Mol Biol Transl Sci. 2017;150:147-56.
8. Berman HM, Westbrook J, Feng Z, Gilliland G, Bhat TN, Weissig H, et al. The Protein Data Bank. Nucleic Acids Res. 2000 Jan 1;28(1):235-42.
9. Dugger BN, Dickson DW. Pathology of Neurodegenerative Diseases. Cold Spring Harb Perspect Biol. 2017 Jul 5;9(7):a028035.
10. Heemels MT. Neurodegenerative diseases. Nature. 2016 Nov 10;539(7628):179.
11. Vaquer-Alicea J, Diamond MI. Propagation of Protein Aggregation in Neurodegenerative Diseases. Annu Rev Biochem. 2019 Jun 20;88:785-810.
12. Lee VM, Goedert M, Trojanowski JQ. Neurodegenerative tauopathies. Annual Review of Neuroscience. 2001 Mar;24(1):1121-59.
13. Schmitz M, Dittmar K, Llorens F, Gelpi E, Ferrer I, Schulz-Schaeffer WJ, et al. Hereditary Human Prion Diseases: an Update. Mol Neurobiol. 2017 Aug;54(6):4138-49.
14. Krzek M, Stroobants S, Gelin P, De Malsche W, Maes D. Influence of Centrifugation and Shaking on the Self-Assembly of Lysozyme Fibrils. Biomolecules. 2022 Nov 24;12(12):1746.
15. Krishnamurthy S, Sudhakar S, Mani E. Kinetics of aggregation of amyloid β under different shearing conditions: Experimental and modelling analyses. Colloids Surf B Biointerfaces. 2022 Jan;209(Pt 1):112156.
16. Roterman I, Stapor K, Fabian P, Konieczny L. In Silico Modeling of the Influence of Environment on Amyloid Folding Using FOD-M Model. Int J Mol Sci. 2021 Sep 30;22(19):10587.
17. Roterman I, Konieczny L. Protein Is an Intelligent Micelle. Entropy (Basel). 2023 May 26;25(6):850.
18. Levitt M. A simplified representation of protein conformations for rapid simulation of protein folding. J Mol Biol. 1976 Jun 14;104(1):59-107.

19. Kalinowska B, Banach M, Konieczny L, Roterman I. Application of divergence entropy to characterize the structure of the hydrophobic core in DNA interacting proteins. Entropy. 2015 Mar 23;17(3):1477-507.

20. Kullback S, Leibler RA. On information and sufficiency. The annals of mathematical statistics. 1951 Mar 1;22(1):79-86.

21. Banach M, Stapor K, Konieczny L, Fabian P, Roterman I. Downhill, Ultrafast and Fast Folding Proteins Revised. Int J Mol Sci. 2020 Oct 15;21(20):7632.

22. Roterman I, Stapor K, Konieczny L. Model of the external force field for the protein folding process-the role of prefoldin. Front Chem. 2024 Mar 26;12:1342434.

23. Roterman I, Stapor K, Konieczny L. Ab initio protein structure prediction: the necessary presence of external force field as it is delivered by Hsp40 chaperone. BMC Bioinformatics. 2023 Nov 7;24(1):418.

24. Roterman I, Stapor K, Dułak D, Konieczny L. External Force Field for Protein Folding in Chaperonins-Potential Application in In Silico Protein Folding. ACS Omega. 2024 Apr 10;9(16):18412-28.

25. Roterman I, Konieczny L, Stapor K, Słupina M. Hydrophobicity-Based Force Field In Enzymes. ACS Omega. 2024 Feb 7;9(7):8188-203.

26. Dygut J, Kalinowska B, Banach M, Piwowar M, Konieczny L, Roterman I. Structural Interface Forms and Their Involvement in Stabilization of Multidomain Proteins or Protein Complexes. Int J Mol Sci. 2016 Oct 18;17(10):1741.

27. Patskovsky Y, Ramagopal U, Toro R, Sauder JM, Dickey M, Iizuka, et al. New York Sgx Research Center For Structural Genomics (Nysgxrc) – PDB.

28. Riek R, Hornemann S, Wider G, Billeter M, Glockshuber R, Wüthrich K. NMR structure of the mouse prion protein domain PrP(121-231). Nature. 1996 Jul 11;382(6587):180-2.

29. Roterman I, Stapor K, Gądek K, Gubała T, Nowakowski P, Fabian P, et al. On the Dependence of Prion and Amyloid Structure on the Folding Environment. Int J Mol Sci. 2021 Dec 16;22(24):13494.

30. Shi W, Munagala NR, Wang CC, Li CM, Tyler PC, Furneaux RH, et al. Crystal structures of Giardia lamblia guanine phosphoribosyltransferase at 1.75 A(,). Biochemistry. 2000 Jun 13;39(23):6781-90.

31. Sato H, Takeda K, Tani K, Hino T, Okada T, Nakasako M, et al. Specific lipid-protein interactions in a novel honeycomb lattice structure of bacteriorhodopsin. Acta Crystallogr D Biol Crystallogr. 1999 Jul;55(Pt 7):1251-6.

32. Wilce MC, Dooley DM, Freeman HC, Guss JM, Matsunami H, McIntire WS, et al. Crystal structures of the copper-containing amine oxidase from Arthrobacter globiformis in the holo and apo forms: implications for the biogenesis of topaquinone. Biochemistry. 1997 Dec 23;36(51):16116-33.

33. Roterman I, Stapor K, Fabian P, Konieczny L. In Silico Modeling of the Influence of Environment on Amyloid Folding Using FOD-M Model. Int J Mol Sci. 2021 Sep 30;22(19):10587.

34. Dułak D, Gadzała M, Banach M, Konieczny L, Roterman I. Alternative Structures of α-Synuclein. Molecules. 2020 Jan 30;25(3):600.

35. Roterman I, Stapor K, Konieczny L. Structural Specificity of Polymorphic Forms of α-Synuclein Amyloid. Biomedicines. 2023 Apr 29;11(5):1324.

36. Banach M, Konieczny L, Roterman I. The Amyloid as a Ribbon-Like Micelle in Contrast to Spherical Micelles Represented by Globular Proteins. Molecules. 2019 Dec 3;24(23):4395.

37. Roterman I, Stapor K, Konieczny L. Secondary Structure in Amyloids in Relation to Their Wild Type Forms. Int J Mol Sci. 2022 Dec 21;24(1):154.

38. Roterman I, Stapor K, Dułak D, Konieczny L. Secondary structure in polymorphic forms of alpha-synuclein amyloids. Acta Biochim Pol. 2023 Jun 18;70(2):435-45.

39. Roterman I, Stapor K, Dułak D, Konieczny L. The Possible Mechanism of Amyloid Transformation Based on the Geometrical Parameters of Early-Stage Intermediate in Silico Model for Protein Folding. Int J Mol Sci. 2022 Aug 22;23(16):9502.

40. Banach M, Roterman I. Solenoid – amyloid under control. In: Roterman-Konieczna I, Editor. From globular proteins to amyloids. Amsterdam: Elsevier; 2020. pp. 95-116.

41. Roterman I, Banach M, Konieczny L. Towards the design of anti-amyloid short peptide helices. Bioinformation. 2018 Jan 31;14(1):1-7.

42. Roterman I, Stapor K, Konieczny L. Transmembrane proteins-Different anchoring systems. Proteins. 2024 May;92(5):593-609.

43. Roterman I, Stapor K, Konieczny L. New insights on the catalytic center of proteins from peptidylprolyl isomerase group based on the FOD-M model. J Cell Biochem. 2023 Jun;124(6):818-35.

44. Roterman I, Stapor K, Konieczny L. Role of environmental specificity in CASP results. BMC Bioinformatics. 2023 Nov 11;24(1):425.

45. Roterman I, Stapor K, Fabian P, Konieczny L. New insights into disordered proteins and regions according to the FOD-M model. PLoS One. 2022 Oct 10;17(10):e0275300.

46. Roterman I, Stapor K, Fabian P, Konieczny L. In Silico Modeling of COVID-19 Pandemic Course Differentiation Using the FOD Model. Coronaviruses. 2022;3:e020622205580.